

Article

Catalytic Performance of Waste-Based Metal Oxides Towards Waste-Based Combustion Process

Notsawan Swadchaipong¹, Vut Tongnan¹, Ammarika Makdee¹ , Unalome Wetwatana Hartley¹ 
and Issara Sereewatthanawut^{2,3,*} 

¹ Department of Chemical Engineering and Management, The Sirindhorn International Thai-German Graduate School of Engineering, King Mongkut's University of Technology North Bangkok, Bangkok 10800, Thailand; notsawan.s@tggs.kmutnb.ac.th (N.S.); vut.t@tggs.kmutnb.ac.th (V.T.); ammarika.dee@gmail.com (A.M.); unalome.w.cpe@tggs-bangkok.org (U.W.H.)

² King Prajadhipok's Institute, Bangkok 10210, Thailand

³ Faculty of Engineering and Technology, Pathumthani University, Pathumthani 12000, Thailand

* Correspondence: issara.se@kpi.ac.th

Abstract: The catalytic performance of mixed metal oxides in the combustion of paper industrial waste (bark, paper sludge, and waste paper reject) was investigated. The mixed metal oxide catalyst with, SiO₂, Al₂O₃, Fe₂O₃, and CaO percentages of 78.57, 9.28, 4.28, and 7.85, respectively, was prepared by mixing iron mill scale, clinker, used cement, and bentonite clay, which were employed as metal oxide precursors. An analysis of the combustion behavior of bark, paper sludge, and waste paper reject with and without a mixed metal oxide catalyst, using the thermogravimetric analysis technique, showed that the ignition temperature remained unchanged after the addition of the catalyst. In contrast, the burnout temperature was reduced from 616.9 to 482.6 °C, 682.0 to 672.5 °C, and 678.1 to 669.9 °C for bark, paper sludge, and waste paper reject, respectively. These results indicated that adding a mixed metal oxide catalyst enhanced the combustion reactivity via the accelerated char combustion of biomass. Furthermore, the products formed during the combustion process with and without a catalyst were investigated in a packed-bed reactor. The gaseous products (H₂, CO, CH₄, C₂H₄, C₂H₆, and CO₂) were observed during the combustion process of bark, paper sludge, and waste paper reject at 700 °C, both with and without a mixed metal oxide catalyst. However, higher H₂ and CO₂ compositions, which are attributed to the catalyst addition, were found in the presence of a catalyst, which improved the tar decomposition and the water–gas shift reaction.

Keywords: combustion; mixed metal oxides; industrial waste; biomass



Academic Editors: Loreta Tamasauskaitė-Tamasiunaite and Virginija Kepeniene

Received: 27 September 2024

Revised: 23 November 2024

Accepted: 25 November 2024

Published: 7 February 2025

Citation: Swadchaipong, N.; Tongnan, V.; Makdee, A.; Hartley, U.W.; Sereewatthanawut, I. Catalytic Performance of Waste-Based Metal Oxides Towards Waste-Based Combustion Process. *Catalysts* **2025**, *15*, 153. <https://doi.org/10.3390/catal15020153>

Copyright: © 2025 by the authors. Licensee MDPI, Basel, Switzerland. This article is an open access article distributed under the terms and conditions of the Creative Commons Attribution (CC BY) license (<https://creativecommons.org/licenses/by/4.0/>).

1. Introduction

Biomass has become an important feedstock for energy generation via combustion, in areas such as boilers or power plants, due to its lower cost compared to conventional fossil-based fuels. Biomass usually contains less carbon, sulfur, and nitrogen and more oxygen, hydrogen, and volatile matter than fossil fuels. Thus, it has a lower carbon footprint. On the other hand, biomass often has a higher moisture content than coal, as the heating value of flue gas in the combustion chamber is low [1,2]. Although biomass generally has less char compared to coal, the biomass char is often much more reactive towards oxidation than any coal char, and, accordingly, the predominant form of biomass combustion is the gas phase oxidation of char via a gasification reaction by O₂, CO₂, and H₂O [3]. The main challenges of biomass combustion include its low heating value, slagging, fouling, and corrosion,

which are the result of moisture content, chlorine, potassium, and phosphorus contained in the biomass. The moisture content is one of the important factors affecting the process' efficiency, as it can require a significant amount of external energy and prolong the starting-up time in the reactor. Orang and Tran [4] studied the effect of biomass moisture content on the performance of a biomass-fed boiler. It was found that more than 30% of the moisture content contained in the biomass resulted in a significant increase in starting-up time (drying the biomass) and ignition time and led to a decrease in the furnace's temperature. However, moisture only has a small influence on the devolatilization rate and the char burning rate. The combustion of biomass is unstable because of its low calorific value and high ash content. Many studies have indicated that the thermal reactivity of biomass or coal can be improved by adding various additives. These additives can be classified as (1) pre-flame additives (to improve the storage and handling of fuel), (2) combustion additives (to improve the combustion efficiency and to reduce pollutants and particulates), and (3) post-flame functioning additives (for particulate collection, fireside deposit control, and cold-side corrosion reduction) [5,6].

Alkaline, alkaline earth, and transition metals in the forms of salts or oxides, (e.g., olivine, kaolin, dolomite, bentonite, CaO, MgO, NiO, K₂CO₃, MnO₂, and Fe₂O₃) were widely applied in the combustion process, and demonstrated high combustion performance by increasing combustion reactivity, reducing the ignition temperature, decreasing the unburnt char, and reducing the pollutants in the exhaust gas [7–9]. Additionally, the metal oxide materials can act as oxygen carriers, which can enhance oxygen transfer behavior due to their oxygen storage and redox properties [10,11]. Z. Wang et al. [12] found that CaO, CeO₂, MnO₂, and Fe₂O₃ catalysts improved combustion activity and accelerated the fixed carbon combustion of the blended fuel (sewage sludge and pulverized coal) by decreasing the ignition temperature and burnout temperature of the fuels. S. Fang et al. [13] discovered that MgO, Al₂O₃, and ZnO contribute to the decrease in the initial temperature and activation energy of the pyrolysis process of paper sludge. Moreover, the effect of an oxide support, such as SiO₂, on catalytic efficiency has been tested, because it produces a higher metallic surface area and a higher sintering resistance [14]. Recently, there have been an increasing number of reports on the preparation of catalysts from earth-abundant and low-cost precursors such as waste materials which are more cost-effective and environmentally friendly.

Therefore, in this work, the combustion behavior of paper industrial waste (bark, paper sludge, and waste paper reject) was investigated with and without the addition of waste-based catalyst. A mixed metal oxide (SiO₂, Al₂O₃, Fe₂O₃, and CaO) catalyst was synthesized using iron mill scale, clinker, used cement, and bentonite clay as metal oxide precursors. The metal oxide precursors were characterized by X-ray fluorescence (XRF) and X-ray diffraction (XRD). The prepared mixed metal oxide catalyst was analyzed using X-ray fluorescence (XRF), N₂ adsorption–desorption, CO₂-temperature programmed desorption (CO₂-TPD), and NH₃-temperature programmed desorption (NH₃-TPD). The combustion behaviors of biomass with and without a catalyst were performed using thermogravimetric analysis (TGA), derivative thermogravimetric analysis (DTG), and differential scanning calorimeter (DSC) techniques. Furthermore, the gaseous products generated during the combustion process were analyzed using a packed-bed reactor and gas chromatography.

2. Results and Discussion

2.1. Biomass and Metal Oxide Precursors Analysis

All waste materials received directly from the industrial paper had a moisture level of more than 50 wt% (55.0, 68.0, and 70.0 wt% for bark, paper sludge, and waste paper reject, respectively). The proximate and ultimate analysis, as well as the calorific values

of the biomass on a dry basis, were examined, and the results were presented in Table 1. The biomass on a dry basis exhibited high amounts of volatiles (60–70 wt%) and low ash content (9–24 wt%). Table 2 shows the metal oxide compositions of clinker, used cement, and bentonite clay using the XRF technique. SiO₂, Al₂O₃, Fe₂O₃, and CaO compositions in clinker were 16.40, 2.87, 3.33, and 75.00 wt%, respectively, while those of used cement were 30.82, 2.38, 2.15, and 41.96 wt%, respectively. For bentonite clay, the SiO₂, Al₂O₃, Fe₂O₃, and CaO compositions were 73.07, 13.10, 6.83, and 1.79 wt%, respectively.

Table 1. Properties of biomass.

	Bark	Paper Sludge	Waste Paper Reject
Proximate analysis (wt%, dry basis)			
Moisture	4.11	7.38	10.95
Ash	9.31	24.00	18.91
Volatile matter	69.90	62.80	64.58
Fixed carbon	16.68	5.82	5.56
Ultimate analysis (wt%, dry basis)			
Carbon	42.00	40.60	43.00
Hydrogen	5.00	5.00	6.00
Oxygen	43.29	28.30	30.85
Nitrogen	0.36	1.80	1.22
Sulfur	0.04	0.30	0.02
Calorific value (MJ/kg, dry basis)			
HHV	18.87	13.18	18.31
LHV	17.53	12.18	17.39

Table 2. Metal oxide compositions of industrial waste precursors.

Metal Oxide	Content (wt%)		
	Clinker	Used Cement	Bentonite Clay
SiO ₂	16.40	30.82	73.07
Al ₂ O ₃	2.87	2.38	13.10
Fe ₂ O ₃	3.33	2.15	6.83
CaO	75.00	41.96	1.79
Other oxides (MgO, SO ₃ , K ₂ O, TiO ₂ , P ₂ O ₅)	1.98	5.71	5.21

The crystal structures of metal oxide precursors (iron mill scale, clinker, used cement, and bentonite clay) were investigated using XRD. Figure 1a shows the peak positions of the iron mill scale (after calcination) at 23.7 (012), 32.7 (104), 35.1 (110), 40.4 (113), 49.0 (024), 53.6 (116), 57.1 (018), 62.0 (214), 63.7 (300), 71.6 (101), and 75.1 (220), which are indexed with the phase of pure hematite iron oxide (α -Fe₂O₃; PDF No. 01-080-5405) [15,16]. The XRD patterns of the clinker (after calcination) are shown in Figure 1b, which exhibited the mixed phases of calcium oxide (CaO; PDF No. 37-1497), tricalcium silicate (3CaO·SiO₂, C₃S), dicalcium silicate (2CaO·SiO₂, C₂S), tricalcium aluminate (3CaO·Al₂O₃, C₃A), and tetracalcium aluminoferrite (4CaO·Al₂O₃·Fe₂O₃, C₄AF) [17,18]. The C₃S is the dominant phase in clinkers, while the other phases (C₂S, C₃A, and C₄AF) highly overlap with C₃S, particularly in the 2 θ range of 27–35°. Figure 1c displays the XRD patterns of the used cement (after calcination), corresponding to the mixed phases of quartz (SiO₂; PDF No. 01-089-8936), calcium oxide (CaO; PDF No. 37-1497), magnesium oxide (MgO; PDF No. 78-0430), tricalcium silicate (3CaO·SiO₂, C₃S), and dicalcium silicate (2CaO·SiO₂, C₂S).

The XRD patterns of the bentonite clay (after calcination) revealed the mixed phases of montmorillonite ($(\text{Na}, \text{Ca})_{0.3}(\text{Al}, \text{Mg})_2\text{Si}_4\text{O}_{10}(\text{OH})_2 \cdot x\text{H}_2\text{O}$; PDF No. 00-003-0015), quartz (SiO_2 ; PDF No. 01-089-8936), and cristobalite (SiO_2 ; PDF No. 00-001-0438), as shown in Figure 1d.

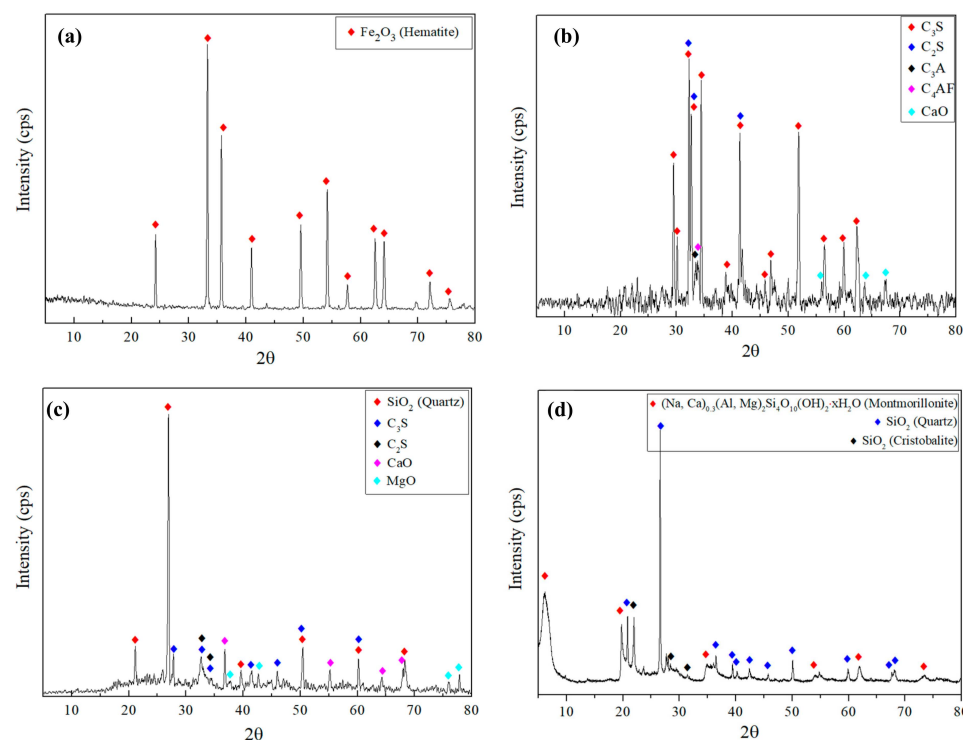


Figure 1. XRD patterns of metal oxide precursors; (a) iron mill scale, (b) clinker, (c) used cement and (d) bentonite clay.

2.2. Mixed Metal Oxide Catalyst Analysis

The compositions of metal oxides in the mixed metal oxide catalyst prepared from the physical mixing of iron mill scale, clinker, used cement, and bentonite clay were determined by XRF. The prepared catalyst consisted of SiO_2 , Al_2O_3 , Fe_2O_3 , and CaO at the percentages of 78.6, 9.3, 4.3, and 7.8 wt%, respectively. The porosity of the prepared catalyst was examined by N_2 physisorption analysis, and the result was revealed in Figure 2. The isotherm with hysteresis loops was observed, corresponding to type IV isotherms in IUPAC classification, indicating the presence of mesoporous structure. The mesoporous structure allows for the rapid and easy diffusion of the reactants during the catalytic processes [19]. The calculated specific surface area and average pore diameter of the prepared catalyst was $15.2 \text{ m}^2/\text{g}$ and 14.71 nm , respectively. Figure 3 shows the CO_2 -TPD profile of the prepared mixed metal oxide catalyst. The small peak at a low temperature ($100\text{--}350 \text{ }^\circ\text{C}$), which can be clearly observed in Figure 3 (inset), was assigned to weak basic sites owing to the physical adsorption of CO_2 on the catalyst surface. The large peak at $800 \text{ }^\circ\text{C}$ indicated strong basic sites which was attributed to the decomposition of CaCO_3 into CO_2 . Therefore, the presence of CaO is conducive to the strong basicity of the catalyst, which may lead to higher CO_2 capture capacity. The amounts of basic sites on the catalyst surface were 58.8 and $981.9 \text{ } \mu\text{g}/\text{g}_{\text{cat}}$ for weak and strong basic sites, respectively. The NH_3 -TPD profile of the catalyst is shown in Figure 4. The NH_3 desorbed from the catalyst surface occurred in a wide peak ranging from 100 to $800 \text{ }^\circ\text{C}$, corresponding to the acid sites, with a total NH_3 quantity of $326.8 \text{ } \mu\text{g}/\text{g}_{\text{cat}}$. The catalytic activity and resistance to coke deposition are significantly influenced by the acidic and basic properties of the catalyst [20]. Enhanced CO_2 adsorption

on the catalyst surface promotes increased CO conversion and H₂ production by effectively shifting the chemical equilibrium of the water–gas shift reaction [21]. Furthermore, it is proposed that acidic sites on the catalyst are suggested to promote coke deposition through hydrocarbon cracking, whereas basic sites contribute to coke removal via coke reforming processes [22]. However, at higher temperatures, the relationship between catalytic activity and catalyst acidity weakens, most likely due to the greater extent of thermal reactions, while the basicity of the catalyst remains beneficial in promoting tar decomposition [23].

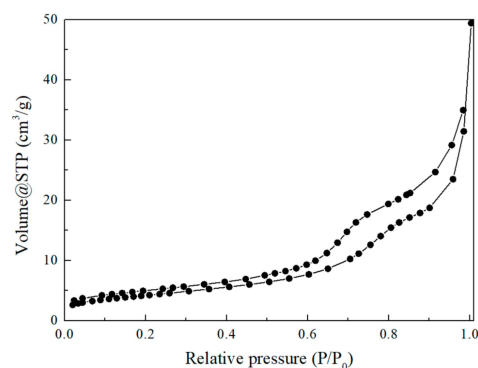


Figure 2. N₂ adsorption–desorption isotherm of the prepared mixed metal oxide catalyst.

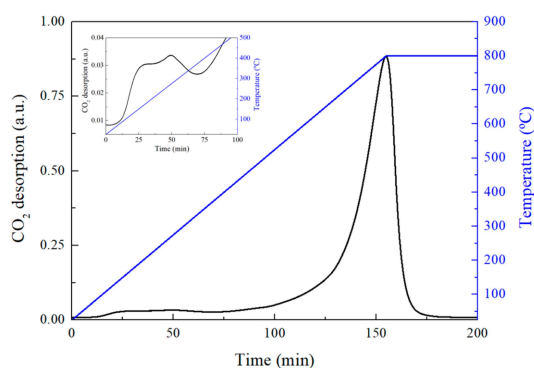


Figure 3. CO₂–TPD profile of the prepared mixed metal oxide catalyst and magnification of CO₂ desorption peak at 100–350 °C (inset).

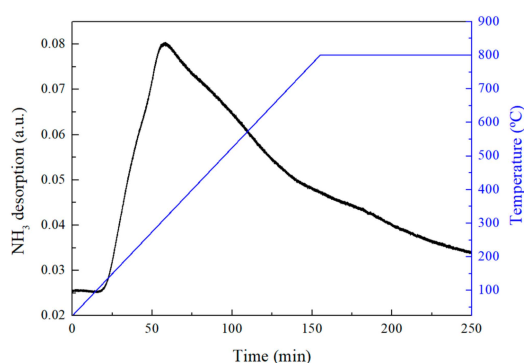


Figure 4. NH₃–TPD profile of the prepared mixed metal oxide catalyst.

2.3. Combustion Behaviors of Biomass Using TG-DTG and DSC Analysis

The combustion behavior of biomass was investigated using the TG-DTG technique under an air atmosphere with a flow rate of 60 mL/min, and the results are illustrated in Figure 5. The DTG curve of bark (Figure 5a) is separated into three stages. The first stage, in the range of 50–200 °C, corresponded to the evaporation of moisture with a mass loss of 12.83 wt%. The second stage was attributed to the volatilization of hemicellulose,

cellulose, and lignin in the temperature ranges of 200–350, 350–430, and 430–510 °C [24–26], respectively, with a total mass loss of 68.37 wt%. The third stage, in the temperature range of 550–650 °C, corresponded to the combustion of residual volatile matter and char, with a mass loss of 3.45 wt%. These three stages were also observed for paper sludge (Figure 5b) and waste paper reject (Figure 5c). However, the combustion behavior of both biomasses differed from that of woody biomass because the paper sludge and waste paper reject were more heterogeneous materials than bark. The third stage, as mentioned above, of paper sludge and waste paper reject extended up to around 700 °C, with mass loss of 7.18 and 5.01 wt%, respectively. For the second stage, which was the volatilization of volatile matter, extreme mass loss was observed in the temperature range of 200–500 °C, with a mass loss of 58.54 and 73.72 wt% for paper sludge and waste paper reject, respectively [27].

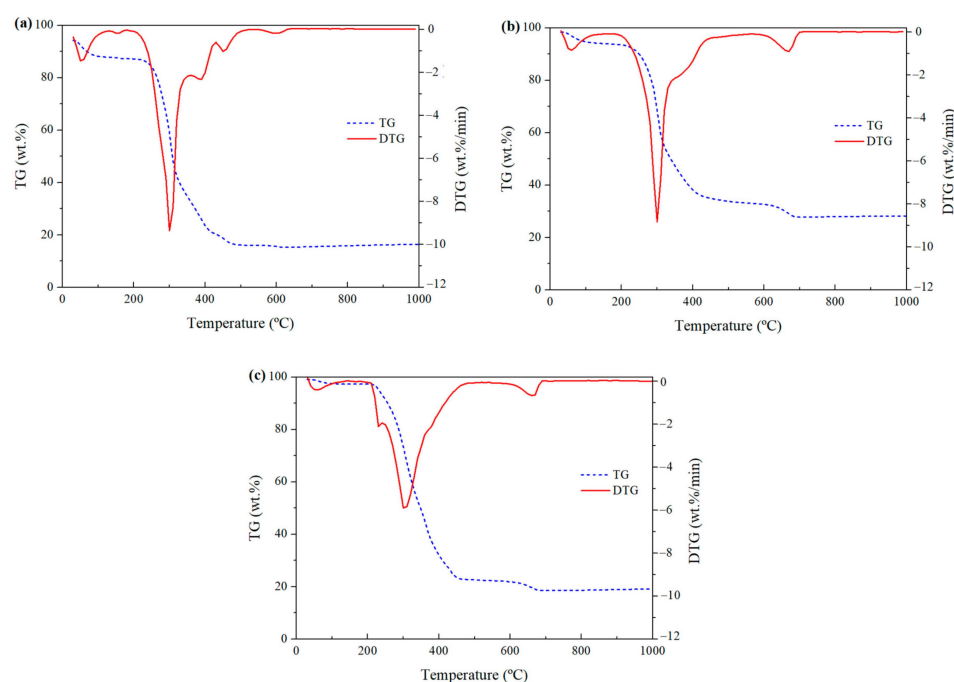


Figure 5. TG–DTG curves of biomass combustion: (a) bark, (b) paper sludge, and (c) waste paper reject.

The combustion characteristic parameters of the biomass, i.e., maximum mass loss rate (DTG_{max}), average mass loss rate (DTG_{mean}), temperature of maximum weight loss rate (T_m), ignition temperature (T_i), burnout temperature (T_b), time of maximum mass loss rate (t_m), ignition time (t_i), burnout time (t_b), time at $DTG/DTG_{max} = 1/2$, ignition index (C_i), burnout index (C_b), and combustibility index (S), are summarized in Table 3. The ignition temperature (T_i) of bark, paper sludge, and waste paper reject were 264.3, 271.8, and 271.8 °C, respectively. The result can be described that a large amount of volatile matter and the energy released by them, as well as the higher H/C ratio (see Table 1), reduced their ignition temperature, due to the ignition temperature depending on the initial release of volatile matter, and on how instantly the heat was released by volatile combustion [10,27].

The burnout temperature (T_b) of biomass is defined as the temperature at which the weight loss rate was less than 1 wt%/min. At this temperature, the combustion was assumed to be almost complete. Normally, a lower burnout temperature suggests that the fuel burned rapidly [28]. Among the biomass, bark showed the lowest burnout temperature at 616.9 °C, which is a generally accepted reason why the lower ash content is an important factor leading to the high burnout index [29]. The burnout index (C_b) is inversely proportional to burnout temperature; lowering the burnout temperature provides

higher burnout efficiency. Additionally, the combustibility index (S) exhibited the same trend as the ignition and burnout index.

Table 3. Combustion characteristic parameters of biomass with and without a catalyst.

	DTG_{max} (%/min)	DTG_{mean} (%/min)	T_m (°C)	T_i (°C)	T_b (°C)	t_m (min)	t_i (min)	t_b (min)	$\Delta t_{1/2}$ (min)	$C_i \times 10^{-2}$ (%/min ³)	$C_b \times 10^{-4}$ (%/min ⁴)	$S \times 10^{-7}$ (% ² /°C ³ min ²)
BA	9.31	2.39	300.5	264.3	616.9	28.0	24.4	59.4	53.8	1.36	1.04	5.17
SL	10.29	2.68	300.5	271.8	682.0	28.0	25.0	66.3	52.1	1.27	0.92	2.62
WR	8.86	1.49	304.7	271.8	678.1	28.4	25.0	65.8	47.9	0.83	0.66	2.23
MM-BA	7.25	1.52	300.5	261.2	482.6	28.0	24.0	46.6	54.3	1.53	1.45	8.39
MM-SL	5.89	1.89	305.9	271.8	672.5	28.6	25.0	65.1	49.2	1.01	0.79	2.22
MM-WR	5.17	1.24	312.9	268.9	669.9	29.3	24.8	65.1	49.4	0.71	0.55	1.32

The biomass combustion, with an addition of a mixed metal oxide catalyst, was also investigated using the TG-DTG profile, as shown in Figure 6. The percentages of residue mass for bark (BA) and paper sludge (SL) combustion with a catalyst were similar to those without a catalyst; however, waste paper reject (WR) with a catalyst was higher than without due to the heterogeneity of the waste paper reject. The combustion characteristics parameters of biomass with a catalyst are also presented in Table 3. When comparing the combustion behavior of biomass with and without a catalyst, the ignition temperature of combustion was not significantly different. Nevertheless, the burnout temperature of bark, paper sludge, and waste paper reject with a catalyst (MM-BA, MM-SL, and MM-WR) decreased from 616.9 to 482.6 °C, 682.0 to 672.5 °C, and 678.1 to 669.9 °C, respectively, compared to those without a catalyst (BA, SL, and WR). It can be indicated that a mixed metal oxide catalyst improved biomass combustion reactivity via accelerated char combustion. This is because the metal oxide acts as an oxygen carrier, which promotes the oxygen transfer to the char [6,10,12,30,31].

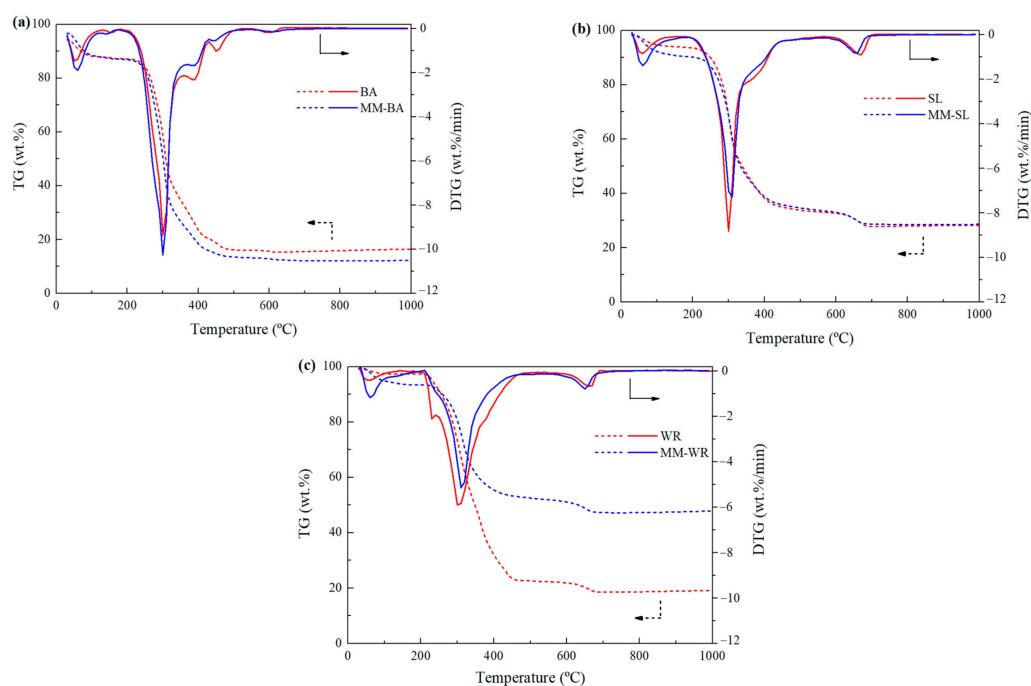


Figure 6. The biomass combustion profile with and without mixed a metal oxide catalyst: (a) bark, (b) paper sludge, and (c) waste paper reject (solid arrow point to DTG value for solid line graph and dashed arrow point to TG value for dashed line graph).

The direction of heat flow during the combustion process as a function of temperature was investigated by the DSC technique, as illustrated in Figure 7. The heat flow of combustion for all biomass, with and without a catalyst, showed two distinct exothermic reaction regions. The first region, at temperatures ranging from 200 to 350 °C, refers to hemicellulose volatilization, while the second region, from 350 to 500 °C, reflects cellulose and lignin combustion. Both regions indicated the reactivity of biomass fuels [32]. The enthalpy for combustion of bark (BA), bark with catalyst (MM-BA), paper sludge (SL), paper sludge with catalyst (MM-SL), waste paper reject (WR), and waste paper reject with catalyst (MM-WR) were 214.8, 248.7, 156.6, 192.3, 280.8, and 135.8 J/g, respectively.

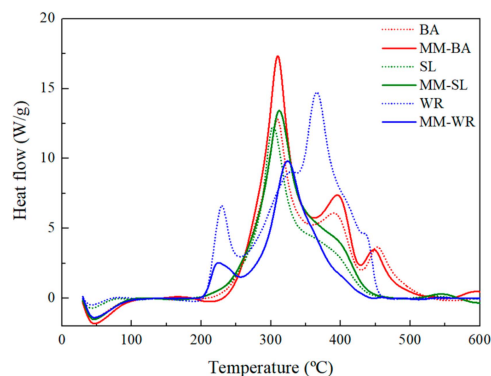


Figure 7. DSC curves of biomass combustion with and without mixed metal oxide catalyst.

2.4. Combustion Behavior of Biomass Using a Packed-Bed Reactor

The combustion process is the most obvious and the oldest method to create energy from biomass. During combustion, material is burned in the presence of oxygen and converted into CO₂ and H₂O while releasing energy. However, the combustion process consists of many overlapping processes: drying, pyrolysis, tar cracking, and gasification. Pyrolysis (Equation (1)) is the thermal degradation of biomass in the absence of oxygen to produce solid, liquid, or gaseous fuels or valuable chemicals. Tar cracking (Equation (2)) is the process of cracking tar molecules into gases, lighter hydrocarbons, char, and steam. Gasification is the process of converting biomass or carbonaceous solids (char) into gaseous products at high temperatures using gasification agents such as air/O₂, H₂O, and CO₂. The gasification process includes oxidation (Equations (3)–(6)), Boudouard (Equation (7)), carbon steam reforming (Equation (8)), methane production (Equation (9)), water–gas shift (Equation (10)), and methane steam reforming (Equation (11)) [33].

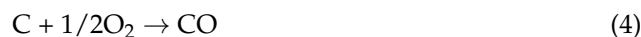
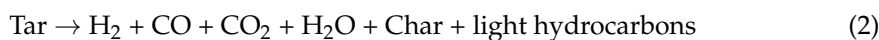




Figure 8 exhibits the formation of gaseous products during the combustion process of bark, paper sludge, and waste paper reject, with and without a mixed metal oxide catalyst at 700 °C using 21%O₂/Ar as an oxidant. The production of H₂, CO, CH₄, C₂H₄, C₂H₆, and CO₂ was detected in all experiments, which corresponded to the products described in Equations (1)–(11). Bark (BA) exhibited the highest reactivity (highest total gas yield) towards the combustion conditions. These results related to the higher combustibility index (Table 3) of bark when compared to paper sludge (SL) and waste paper reject (WR). The addition of the catalyst boosted the total gas production, due to a significant rise in CO₂ and H₂ concentrations. This could be due to the thermochemical reactions between char, tar, and Fe₂O₃, Al₂O₃, and CaO in the catalyst, as follows:

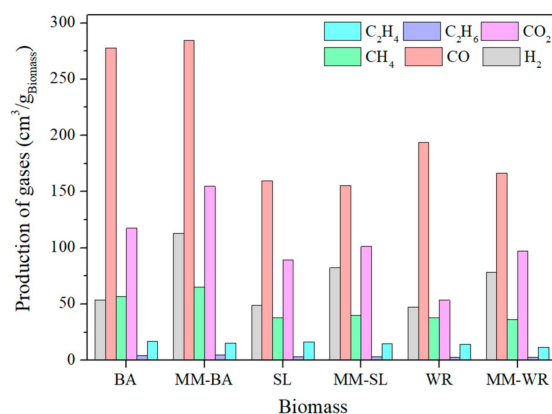
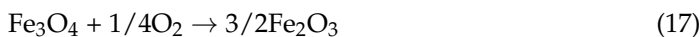
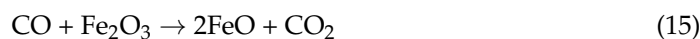


Figure 8. Production of gaseous products from the combustion process of bark, paper sludge, and waste paper reject at 700 °C with (MM-BA, MM-SL, and MM-WR) and without (BA, SL, and WR) mixed metal oxide catalyst.

(1) Iron oxide (Fe₂O₃) acts as an oxygen carrier, promoting biomass tar conversion (Equation (2)) and char gasification (Equations (12)–(14)). The produced CO was then catalytically converted to H₂ and CO₂ via a water–gas shift process (Equations (15) and (16)) [34]. The produced Fe₃O₄ can be oxidized to produce active Fe₂O₃ (Equation (17)).



(2) The addition of Al₂O₃ in the catalyst greatly improved the activity of the Fe₂O₃ catalyst for the decomposition and gasification of biomass tar [34].

(3) CaO is a well-known CO₂ adsorbent that interacts with CO₂ to form CaCO₃, as shown in Equation (18), leading to the in situ removal of CO₂ during biomass gasification, driving the chemical equilibrium shift to produce a higher quantity of H₂ [33].



3. Material and Methods

3.1. Biomass and Catalyst Preparations

Different biomass materials from paper industrial waste, i.e., bark, paper sludge and waste paper reject, were provided by Siam Kraft Industry Co., Ltd. (Wangsala, Kan-
chanaburi, Thailand). The source of various metal oxide precursors is industrial waste, i.e.,
clinker, used cement, bentonite clay, and iron mill scale. All industrial waste precursors
were crushed and then calcined at 900 °C (10 °C/min) for 2 h under 21%O₂/Ar for iron
mill scale and calcined in air at 700 °C (10 °C/min) for 12 h for clinker, used cement and
bentonite clay. Mixed metal oxide catalyst was prepared via physical mixing of metal oxide
precursors, including iron mill scale, clinker, used cement, and bentonite clay with the
compositions of SiO₂, Al₂O₃, Fe₂O₃, and CaO at 78.6, 9.3, 4.3, and 7.8 wt%, respectively.
Finally, the mixed metal oxide was calcined in air at 900 °C for 4 h.

3.2. Characterizations

Biomass are characterized by proximate and ultimate analyses. The proximate analysis
gives the content of moisture, volatile, fixed carbon, and ash. The ultimate analysis gives
the composition of elements such as carbon, hydrogen, oxygen, sulfur, and nitrogen. The
crystalline structures of metal oxide precursors, i.e., iron mill scale, clinker, used cement,
and bentonite clay, were characterized using X-ray diffraction (XRD). The metal oxide
compositions in clinker, used cement, bentonite clay, and mixed metal oxide catalyst were
determined using X-ray fluorescence (XRF). The N₂ adsorption–desorption isotherm of a
mixed metal oxide catalyst was measured at −196 °C, and the specific surface area was
calculated by the multiple-point Brunauer–Emmett–Teller (BET) method. The acidity and
basicity of the catalyst were characterized using NH₃ and CO₂-temperature programmed
desorption (TPD), respectively. Before the TPD process, the catalyst was pretreated at
150 °C for 1 h with a flow rate of 100 mL/min of Ar. After that, the catalyst was exposed to
50 mL/min of 5% NH₃/Ar at 50 °C for NH₃-TPD or 100 mL/min of 5% CO₂/Ar at 100 °C
for CO₂-TPD. During the TPD process, the temperature of the catalyst increased from room
temperature to 800 °C, with a heating rate of 5 °C/min under Ar flow of 100 mL/min. The
gases (NH₃ or CO₂) desorption profiles were measured in real time by a mass spectrometer
(GSD 320, OmniStar, Puchheim, Germany).

3.3. Combustion Behavior Using Thermogravimetric Analysis

Biomass combustion was performed in a thermogravimetric analyzer (TGS/DSC3 +
Metler Toledo) and the sample weight loss and rate of weight loss were plotted as functions
of time or temperature. The sample (about 4 mg) was spread uniformly in the crucible,
and the temperature was increased at a rate of 10 °C/min from room temperature to
1000 °C under an air atmosphere (60 mL/min). To investigate the effect of catalyst addition
on biomass combustion performance, the biomass/catalyst weight ratio of 1:1 was used.
The combustion of biomass without a catalyst was labeled BA, SL, and WR, whereas the
combustion with a catalyst was labeled MM-BA, MM-SL, and MM-WR for bark, paper
sludge, and waste paper reject, respectively.

The combustion parameters, i.e., ignition temperature (T_i), burnout temperature (T_b),
and maximum weight loss rate temperature (T_m), were directly obtained from the TG-DTG
thermogram, as illustrated in Figure 9. The combustion parameters were employed to cal-
culate the combustion performance of the fuels using Equations (19)–(21) [12]. The ignition
index (C_i) indicates the reactivity of fuel in the early stages of combustion. The burnout
index (C_b) is used to evaluate the burnout performance. Moreover, the combustibility index
(S) represents the combustion performances of the fuels during the whole combustion

process. The higher ignition, burnout, and combustibility indexes indicates better ignition, burnout, and combustion reactivity, respectively [35].

$$C_i = \frac{DTG_{max}}{t_i t_m} \quad (19)$$

$$C_b = \frac{DTG_{max}}{\Delta t_{1/2} t_m t_b} \quad (20)$$

$$S = \frac{DTG_{max} DTG_{mean}}{T_i^2 T_b} \quad (21)$$

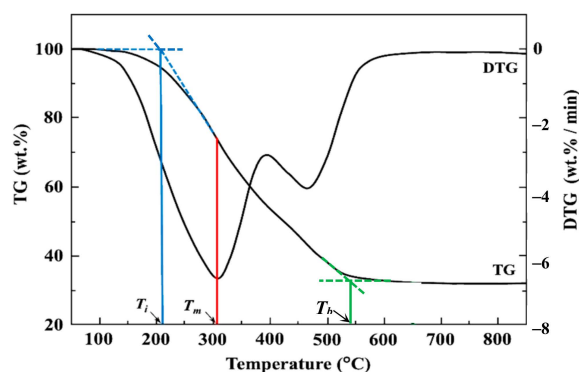


Figure 9. The demonstration plot for determination of ignition temperature (T_i), burnout temperature (T_b), and maximum weight loss rate temperature (T_m).

The variables DTG_{max} , DTG_{mean} , t_i , t_b , t_m , and $\Delta t_{1/2}$ represent maximum mass loss rate, average mass loss rate, ignition time, burnout time, time at maximum mass loss rate, and time at $DTG/DTG_{max} = 1/2$, respectively.

3.4. Combustion Behavior Using a Packed-Bed Reactor

The catalytic combustion of biomass was carried out using a quartz tube packed-bed reactor. An amount of 1.0 g of catalyst was placed into the quartz tube reactor. The reactor temperature was controlled by furnace and monitored using a thermocouple. An amount of 1.0 g of biomass was pelletized and put in a biomass feeder above the reactor. The reactor was heated to 700 °C, under 21%O₂/Ar flow. After the reactor temperature was reached, the biomass in the feeder was fed into the reactor. The gaseous products were collected in a 5 L Tedlar gas sample bag for 45 min before being analyzed using a gas chromatograph (GC). Biomass combustion without a catalyst was also performed in the same procedure, but with quartz sand instead of the catalyst.

4. Conclusions

The biomass materials from paper industrial waste, i.e., bark, paper sludge, and waste paper reject, were characterized by proximate and ultimate analysis. All biomasses have high moisture, volatile matter, and oxygen content. The combustion behaviors of biomass were divided into three stages; the first stage (50–200 °C) was attributed to drying, the second stage (200–500 °C) was devolatilization, and the third stage (500–700 °C) was residual volatile and char burning. The ignition, burnout, and combustibility indexes were used to indicate the combustion reactivity of biomass, with the higher ignition, burnout, and combustibility indexes resulting in better ignition, burnout and combustion reactivity, respectively. These values are related to the compositions of biomass, such as the amount of volatile matter and the H/C ratio. The addition of a mixed metal oxide catalyst, which was prepared from the physical mixing of industrial waste, i.e., clinker, used cement, bentonite

clay, and iron mill scale with the percentages of SiO₂, Al₂O₃, Fe₂O₃, and CaO of 78.57, 9.28, 4.28, and 7.85, has no significant effect on ignition temperature of biomass. However, the burnout temperature of biomass with a catalyst was reduced from 616.9 to 482.6 °C, 682.0 to 672.5 °C, and 678.1 to 669.9 °C for bark, paper sludge, and waste paper reject, respectively, when compared to that without a catalyst. These results indicated that the mixed metal oxide catalyst addition enhanced combustion reactivity via the accelerated char combustion of biomass. Furthermore, the products produced during the combustion process, with and without a catalyst, were investigated using a packed-bed reactor. The production of gases, including H₂, CO, CH₄, C₂H₄, C₂H₆, and CO₂, was observed during the combustion process of bark, paper sludge, and waste paper reject at 700 °C, both with and without mixed metal oxide catalyst. However, higher compositions of H₂ and CO₂ were found in the presence of catalyst which are attributed to the catalyst addition improved the tar decomposition and water-gas shift reaction.

Author Contributions: N.S.: writing—original draft, validation, project administration, conceptualization. V.T.: validation, methodology, investigation, formal analysis. A.M.: writing—editing, visualization, investigation, formal analysis, data curation. U.W.H.: writing—review and editing, supervision, resources, project administration, funding acquisition, conceptualization. I.S.: writing—review and editing, supervision, resources, project administration, funding acquisition, conceptualization. All authors have read and agreed to the published version of the manuscript.

Funding: This research has received funding support from the NRCT (contract number N41A640254 & N83A670023), King Mongkut's University of Technology North Bangkok (contract number KMUTNB-FF-66-52), and NSRF via the Program Management Unit for Human Resources & Institutional Development, Research and Innovation (contact number B48G660108).

Data Availability Statement: The data that support the findings of this study are available on request.

Conflicts of Interest: The authors declare no conflicts of interest.

References

1. Liu, L.; Memon, M.Z.; Xie, Y.; Gao, S.; Guo, Y.; Dong, J.; Gao, Y.; Li, A.; Ji, G. Recent Advances of Research in Coal and Biomass Co-Firing for Electricity and Heat Generation. *Circ. Econ.* **2023**, *2*, 100063. [[CrossRef](#)]
2. Gil, M.V.; Rubiera, F. *Coal and Biomass Cofiring: Fundamentals and Future Trends*; Suárez-Ruiz, I., Diez, M.A., Rubiera, F., Eds.; Woodhead Publishing: Oviedo, Spain, 2019; ISBN 978-0-08-102201-6.
3. Hupa, M.; Karlström, O.; Vainio, E. Biomass Combustion Technology Development—It Is All about Chemical Details. *Proc. Combust. Inst.* **2017**, *36*, 113–134. [[CrossRef](#)]
4. Orang, N.; Tran, H. Effect of Feedstock Moisture Content on Biomass Boiler Operation. *Tappi J.* **2015**, *14*, 629–637. [[CrossRef](#)]
5. Dorner, R.W.; Srinivasan, N.; Shah, J.; Chen, H.-T. Method for Reducing Slag in Biomass Combustion. U.S. Patent No. 20120312206, 13 December 2012.
6. Hu, Y.; Wang, Z.; Cheng, X.; Liu, M.; Ma, C. Effects of Catalysts on Combustion Characteristics and Kinetics of Coal-Char Blends. *IOP Conf. Ser. Earth Environ. Sci.* **2018**, *133*, 012023. [[CrossRef](#)]
7. Zou, C.; Wen, L.; Zhang, S.; Bai, C.; Yin, G. Evaluation of Catalytic Combustion of Pulverized Coal for Use in Pulverized Coal Injection (PCI) and Its Influence on Properties of Unburnt Chars. *Fuel Process. Technol.* **2014**, *119*, 136–145. [[CrossRef](#)]
8. Ueda, S.; Watanabe, K.; Inoue, R.; Ariyama, T. Catalytic Effect of Fe, CaO and Molten Oxide on the Gasification Reaction of Coke and Biomass Char. *ISIJ Int.* **2011**, *51*, 1262–1268. [[CrossRef](#)]
9. Zhang, S.; Chen, Z.D.; Chen, X.J.; Gong, X.Z. Effects of Ash/K₂CO₃/Fe₂O₃ on Ignition Temperature and Combustion Rate of Demineralized Anthracite. *J. Fuel Chem. Technol.* **2014**, *42*, 166–174. [[CrossRef](#)]
10. Vamvuka, D.; Tsamourgeli, V.; Galetakis, M. Study on Catalytic Combustion of Biomass Mixtures with Poor Coals. *Combust. Sci. Technol.* **2014**, *186*, 68–82. [[CrossRef](#)]
11. Nzihou, A.; Stanmore, B.; Sharrock, P. A Review of Catalysts for the Gasification of Biomass Char, with Some Reference to Coal. *Energy* **2013**, *58*, 305–317. [[CrossRef](#)]
12. Wang, Z.; Hong, C.; Xing, Y.; Li, Y.; Feng, L.; Jia, M. Combustion Behaviors and Kinetics of Sewage Sludge Blended with Pulverized Coal: With and without Catalysts. *Waste Manag.* **2018**, *74*, 288–296. [[CrossRef](#)]

13. Fang, S.; Yu, Z.; Lin, Y.; Lin, Y.; Fan, Y.; Liao, Y.; Ma, X. Effects of Additives on the Co-Pyrolysis of Municipal Solid Waste and Paper Sludge by Using Thermogravimetric Analysis. *Bioresour. Technol.* **2016**, *209*, 265–272. [[CrossRef](#)] [[PubMed](#)]
14. Blanco, P.H.; Wu, C.; Onwudili, J.A.; Williams, P.T. Characterization and Evaluation of Ni/SiO₂ Catalysts for Hydrogen Production and Tar Reduction from Catalytic Steam Pyrolysis-Reforming of Refuse Derived Fuel. *Appl. Catal. B Environ.* **2013**, *134–135*, 238–250. [[CrossRef](#)]
15. Wahab, R.; Khan, F.; Al-Khedhairi, A.A. Hematite Iron Oxide Nanoparticles: Apoptosis of Myoblast Cancer Cells and Their Arithmetical Assessment. *RSC Adv.* **2018**, *8*, 24750–24759. [[CrossRef](#)]
16. Park, C.; Jung, J.; Lee, C.W.; Cho, J. Synthesis of Mesoporous α -Fe₂O₃ Nanoparticles by Non-Ionic Soft Template and Their Applications to Heavy Oil Upgrading. *Sci. Rep.* **2016**, *6*, 39136. [[CrossRef](#)] [[PubMed](#)]
17. Zhutovsky, S.; Shishkin, A. Recycling of Hydrated Portland Cement Paste into New Clinker. *Constr. Build. Mater.* **2021**, *280*, 122510. [[CrossRef](#)]
18. Yang, Z.; Zhang, Y.; Liu, L.; Seetharaman, S.; Wang, X.; Zhang, Z. Integrated Utilization of Sewage Sludge and Coal Gangue for Cement Clinker Products: Promoting Tricalcium Silicate Formation and Trace Elements Immobilization. *Materials* **2016**, *9*, 275. [[CrossRef](#)]
19. Wang, J.; Zhang, S.; Xu, D.; Zhang, H. Catalytic Activity Evaluation and Deactivation Progress of Red Mud/Carbonaceous Catalyst for Efficient Biomass Gasification Tar Cracking. *Fuel* **2022**, *323*, 124278. [[CrossRef](#)]
20. Mazumder, J.; De Lasa, H. Fluidizable Ni/La₂O₃-Al₂O₃ Catalyst for Steam Gasification of a Cellulosic Biomass Surrogate. *Appl. Catal. B Environ.* **2014**, *160–161*, 67–79. [[CrossRef](#)]
21. Yang, S.; Zhang, X.; Chen, L.; Yuan, Q.; Sun, L.; Xie, X.; Zhao, B.; Si, H. Characteristics and Catalytic Properties of Bi-Functional Fe/CaO Catalyst for Syngas Production from Pyrolysis of Biomass. *J. Biobased Mater. Bioenergy* **2017**, *10*, 415–422. [[CrossRef](#)]
22. Mazumder, A.S.M.J.I. Steam Gasification of Biomass Surrogates: Catalyst Development and Kinetic Modelling. Ph.D. Thesis, The University of Western Ontario Supervisor, London, ON, Canada, 2014.
23. Viinikainen, T.; Rönkkönen, H.; Bradshaw, H.; Stephenson, H.; Airaksinen, S.; Reinikainen, M.; Simell, P.; Krause, O. Acidic and Basic Surface Sites of Zirconia-Based Biomass Gasification Gas Clean-up Catalysts. *Appl. Catal. A Gen.* **2009**, *362*, 169–177. [[CrossRef](#)]
24. Wyasu, G.; Gimba, C.E.; Agbaji, E.B.; Ndukwe, G.I. Thermo-Gravimetry(TGA) and DSC of Thermal Analysis Techniques in Production of Active Carbon from Lignocellulosic Materials. *Pelagia Res. Libr. Adv. Appl. Sci. Res.* **2016**, *7*, 109–115.
25. Bryś, A.; Bryś, J.; Ostrowska-Ligeza, E.; Kaleta, A.; Górnicki, K.; Głowacki, S.; Koczoń, P. Wood Biomass Characterization by DSC or FT-IR Spectroscopy. *J. Therm. Anal. Calorim.* **2016**, *126*, 27–35. [[CrossRef](#)]
26. Müsellim, E.; Tahir, M.H.; Ahmad, M.S.; Ceylan, S. Thermokinetic and TG/DSC-FTIR Study of Pea Waste Biomass Pyrolysis. *Appl. Therm. Eng.* **2018**, *137*, 54–61. [[CrossRef](#)]
27. Vamvuka, D.; Sfakiotakis, S. Combustion Behaviour of Biomass Fuels and Their Blends with Lignite. *Thermochim. Acta* **2011**, *526*, 192–199. [[CrossRef](#)]
28. Okoroigwe, E.C.; Enibe, S.O.; Onyegegbu, S.O. Determination of Oxidation Characteristics and Decomposition Kinetics of Some Nigerian Biomass. *J. Energy S. Afr.* **2016**, *27*, 39–49. [[CrossRef](#)]
29. Yang, S.; Lei, M.; Li, M.; Liu, C.; Xue, B.; Xiao, R. Comprehensive Estimation of Combustion Behavior and Thermochemical Structure Evolution of Four Typical Industrial Polymeric Wastes. *Energies* **2022**, *15*, 2487. [[CrossRef](#)]
30. Zhang, L.; Duan, F.; Huang, Y. Effect of Organic Calcium Compounds on Combustion Characteristics of Rice Husk, Sewage Sludge, and Bituminous Coal: Thermogravimetric Investigation. *Bioresour. Technol.* **2015**, *181*, 62–71. [[CrossRef](#)]
31. Gong, X.; Guo, Z.; Wang, Z. Reactivity of Pulverized Coals during Combustion Catalyzed by CeO₂ and Fe₂O₃. *Combust. Flame* **2010**, *157*, 351–356. [[CrossRef](#)]
32. Kok, M.V.; Özgür, E. Thermal Analysis and Kinetics of Biomass Samples. *Fuel Process. Technol.* **2013**, *106*, 739–743. [[CrossRef](#)]
33. Narnaware, S.L.; Panwar, N.L. Catalysts and Their Role in Biomass Gasification and Tar Abatement: A Review. *Biomass Convers. Biorefinery* **2021**. [[CrossRef](#)]
34. Azhar Uddin, M.; Tsuda, H.; Wu, S.; Sasaoka, E. Catalytic Decomposition of Biomass Tars with Iron Oxide Catalysts. *Fuel* **2008**, *87*, 451–459. [[CrossRef](#)]
35. Wang, X.D.; Xue, J.J.; Zhu, Y.J.; Liu, C.R.; Hu, X.Y.; Liang, H.; Dong, C.Q. The Study of Combustion Characteristics of Corn Stalks and Cobs via TGA-DTG-DSC Analysis. *IOP Conf. Ser. Earth Environ. Sci.* **2019**, *354*, 012130. [[CrossRef](#)]

Disclaimer/Publisher’s Note: The statements, opinions and data contained in all publications are solely those of the individual author(s) and contributor(s) and not of MDPI and/or the editor(s). MDPI and/or the editor(s) disclaim responsibility for any injury to people or property resulting from any ideas, methods, instructions or products referred to in the content.